Title
Inclusive Λc+ production in e+e- annihilations at s=10.54 GeV and in Υ(4S) decays

Journal
Physical Review D, 75(1)

ISSN
2470-0010

Authors
Aubert, B
Bona, M
Boutigny, D
et al.

Publication Date
2007

DOI
10.1103/physrevd.75.012003

Inclusive Λ_c^+ production in e^+e^- annihilations at $\sqrt{s} = 10.54$ GeV and in $\Upsilon(4S)$ decays

B. Aubert,[1] M. Bona,[1] D. Boutigny,[1] F. Couderc,[1] Y. Karyotakis,[1] J. P. Lees,[1] V. Poireau,[1] V. Tisserand,[1] A. Zghiche,[1] E. Grauges,[2] A. Palano,[3] J. C. Chen,[4] N. D. Qi,[4] G. Rong,[4] P. Wang,[4] Y. S. Zhu,[4] G. Eigen,[5] I. Ofte,[5] B. Stugu,[5] G. S. Abrams,[6] M. Battaglia,[6] D. N. Brown,[6] J. Button-Shafer,[6] R. N. Cahn,[6] E. Charles,[6] M. S. Gill,[6] Y. Groysman,[6] R. G. Jacobsen,[6] J. A. Kadyk,[6] L. T. Kerth,[6] Yu. G. Kolomensky,[6] G. Kukartsev,[6] G. Lynch,[6] L. M. Mir,[6] T. J. Orimoto,[6] M. Pripstein,[6] N. A. Roe,[6] M. T. Ronan,[6] W. A. Wenzel,[6] P. del Amo Sanchez,[7] M. Barrett,[7] K. E. Ford,[7] T. J. Harrison,[7] A. J. Hart,[7] C. M. Hawkes,[7] A. T. Watson,[7] T. Held,[8] H. Koch,[8] B. Lewandowski,[8] M. Pelizaeus,[8] K. Peters,[8] T. Schroeder,[8] M. Steinke,[8] J. T. Boyd,[9] J. P. Burke,[9] W. N. Cottingham,[9] D. Walker,[9] D. J. Asgeirsson,[10] T. Cuhadar-Donszelmann,[10] B. G. Fulsom,[10] C. Hearty,[10] N. S. Knecht,[10] T. S. Mattison,[10] J. A. McKenna,[10] A. Khan,[11] P. Kyberd,[11] M. Saleem,[11] D. J. Sherwood,[11] L. Teodorescu,[11] V. E. Blinov,[12] A. D. Bukin,[12] V. P. Druzhinin,[12] V. B. Golubev,[12] A. P. Onuchin,[12] S. I. Serednyakov,[12] Yu. I. Skovpen,[12] E. P. Solodov,[12] K. Yu Todyshev,[12] M. Bondioli,[13] M. Bruinsma,[13] M. Chao,[13] S. Curry,[13] I. Eschrich,[13] D. Kirkby,[13] A. J. Lankford,[13] P. Lund,[13] M. Mandelkern,[13] R. K. Mommsen,[13] W. Roethel,[13] D. P. Stoker,[13] S. Abachi,[14] C. Buchanan,[14] S. D. Foulkes,[15] J. W. Gary,[15] O. Long,[15] B. C. Shen,[15] K. Wang,[15] L. Zhang,[15] H. K. Hadavand,[16] E. J. Hill,[16] H. P. Paar,[16] S. Rahatlou,[16] V. Sharma,[16] J. W. Berryhill,[17] C. Campagnari,[17] A. Cunha,[17] B. Dahmes,[17] T. M. Hong,[17] D. Kovalskyi,[17] J. D. Richman,[17] T. W. Beck,[18] A. M. Eisner,[18] C. J. Flacco,[18] C. A. Heusch,[18] J. Kroseberg,[18] W. S. Lockman,[18] G. Nesom,[18] T. Schalk,[18] B. A. Schumm,[18] A. Seiden,[18] P. Spradlin,[18] D. C. Williams,[18] M. G. Wilson,[18] J. Albert,[19] E. Chen,[19] A. Dvoretskii,[19] F. Fang,[19] D. G. Hitlin,[19] I. Narsky,[19] T. Piatenko,[19] F. C. Porter,[19] A. Ryd,[19] G. Mancinelli,[20] B. T. Meadows,[20] K. Mishra,[20] M. D. Sokoloff,[20] F. Blanc,[21] P. C. Bloom,[21] S. Chen,[21] W. T. Ford,[21] J. F. Hirschauer,[21] A. Kreisel,[21] M. Nagel,[21] U. Nauenberg,[21] A. Olivas,[21] W. O. Ruddick,[21] J. G. Smith,[21] K. A. Ulmer,[21] S. R. Wagner,[21] J. Zhang,[21] A. Chen,[22] E. A. Eckhart,[22] A. Soffer,[22] W. H. Toki,[22] R. J. Wilson,[22] F. Winklmeier,[22] Q. Zeng,[22] D. D. Altenburg,[23] E. Feltresi,[23] A. Hauke,[23] H. Jasper,[23] J. Merkel,[23] A. Petzold,[23] B. Spaan,[23] T. Brandt,[24] V. Klose,[24] H. M. Lacker,[24] W. F. Mader,[24] R. Nogowski,[24] J. Schubert,[24] K. R. Schubert,[24] R. Schwierz,[24] J. E. Sundermann,[24] A. Volk,[24] D. Bernard,[25] G. R. Bonneaud,[25] E. Latour,[25] Ch. Thiebaux,[25] M. Verderi,[25] P. J. Clark,[26] W. Gradl,[26] F. Muheim,[26] S. Playfer,[26] A. I. Robertson,[26] Y. Xie,[26] M. Andreotti,[27] D. Bettoni,[27] C. Bozzi,[27] R. Calabrese,[27] G. Cibinetto,[27] E. Luppi,[27] M. Negrini,[27] A. Petrella,[27] L. Piemontese,[27] E. Prencipe,[27] F. Anulli,[28] R. Baldini-Ferroli,[28] A. Calcaterra,[28] R. de Sangro,[28] G. Finocchiaro,[28] S. Pacetti,[28] P. Patteri,[28] I. M. Peruzzi,[28,*] M. Piccolo,[28] M. Rama,[28] A. Zallo,[28] A. Buzzo,[29] R. Contri,[29] M. Lo Vetere,[29] M. M. Macri,[29] M. R. Monge,[29] S. Passaggio,[29] C. Patrignani,[29] E. Robutti,[29] A. Santroni,[29] S. Tosi,[29] G. Brandenburg,[30] K. S. Chaisanguanthum,[30] M. Morii,[30] J. Wu,[30] R. S. Dubitzky,[31] J. Marks,[31] S. Schenk,[31] U. Uwer,[31] D. J. Bard,[32] W. Bhimji,[32] D. A. Bowerman,[32] P. D. Dauncey,[32] U. Egede,[32] R. L. Flack,[32] J. A. Nash,[32] M. B. Nikolich,[32] W. Panduro Vazquez,[32] P. K. Behera,[33] X. Chai,[33] M. J. Charles,[33] U. Mallik,[33] N. T. Meyer,[33] V. Ziegler,[33] J. Cochran,[34] H. B. Crawley,[34] L. Dong,[34] V. Eyges,[34] W. T. Meyer,[34] S. Prell,[34] E. I. Rosenberg,[34] A. E. Rubin,[34] A. V. Gritsan,[35] A. G. Denig,[36] M. Fritsch,[36] G. Schott,[36] N. Arnaud,[37] M. Davier,[37] G. Grosdidier,[37] A. Höcker,[37] F. Le Diberder,[37] V. Lepeltier,[37] A. M. Lutz,[37] A. Oyanguren,[37] S. Pruvot,[37] S. Rodier,[37] P. Roudeau,[37] M. H. Schune,[37] A. Stocchi,[37] W. F. Wang,[37] G. Wormser,[37] C. H. Cheng,[38] D. J. Lange,[38] D. M. Wright,[38] C. A. Chavez,[39] I. J. Forster,[39] J. R. Fry,[39] E. Gabathuler,[39] R. Gamet,[39] K. A. George,[39] D. E. Hutchcroft,[39] D. J. Payne,[39] K. C. Schofield,[39] C. Touramanis,[39] A. J. Bevan,[40] F. Di Lodovico,[40] W. Menges,[40] R. Sacco,[40] G. Cowan,[41] H. U. Flaecher,[41] D. A. Hopkins,[41] P. S. Jackson,[41] T. R. McMahon,[41] S. Ricciardi,[41] F. Salvatore,[41] A. C. Wren,[41] D. N. Brown,[42] C. L. Davis,[42] J. Allison,[43] N. R. Barlow,[43] R. J. Barlow,[43] Y. M. Chia,[43] C. L. Edgar,[43] G. D. Lafferty,[43] M. T. Naisbit,[43] J. C. Williams,[43] J. I. Yi,[43] C. Chen,[44] W. D. Hulsbergen,[44] A. Jawahery,[44] C. K. Lae,[44] D. A. Roberts,[44] G. Simi,[44] G. Blaylock,[45] C. Dallapiccola,[45] S. S. Hertzbach,[45] X. Li,[45] T. B. Moore,[45] S. Saremi,[45] H. Staengle,[45] R. Cowan,[46] G. Sciolla,[46] S. J. Sekula,[46] M. Spitznagel,[46] F. Taylor,[46] R. K. Yamamoto,[46] H. Kim,[47] S. E. Mclachlin,[47] P. M. Patel,[47] S. H. Robertson,[47] A. Lazzaro,[48] V. Lombardo,[48] F. Palombo,[48] J. M. Bauer,[49] L. Cremaldi,[49] V. Eschenburg,[49] R. Godang,[49] R. Kroeger,[49] D. A. Sanders,[49] D. J. Summers,[49] H. W. Zhao,[49] S. Brunet,[50] D. Côté,[50] M. Simard,[50] P. Taras,[50] F. B. Viaud,[50] H. Nicholson,[51] N. Cavallo,[52,†] G. De Nardo,[52] F. Fabozzi,[52,†] C. Gatto,[52] L. Lista,[52] D. Monorchio,[52] P. Paolucci,[52] D. Piccolo,[52] C. Sciacca,[52] M. A. Baak,[53] G. Raven,[53] H. L. Snoek,[53] C. P. Jessop,[54] J. M. LoSecco,[54] T. Allmendinger,[55] G. Benelli,[55] L. A. Corwin,[55] K. K. Gan,[55] K. Honscheid,[55] D. Hufnagel,[55] P. D. Jackson,[55] H. Kagan,[55] R. Kass,[55] A. M. Rahimi,[55] J. J. Regensburger,[55] R. Ter-Antonyan,[55] Q. K. Wong,[55] N. L. Blount,[56] J. Brau,[56] R. Frey,[56] O. Igonkina,[56] J. A. Kolb,[56] M. Lu,[56] R. Rahmat,[56] N. B. Sinev,[56] D. Strom,[56] J. Strube,[56] E. Torrence,[56] A. Gaz,[57] M. Margoni,[57] M. Morandin,[57] A. Pompili,[57] M. Posocco,[57] M. Rotondo,[57] F. Simonetto,[57] R. Stroili,[57] C. Voci,[57] M. Benayoun,[58] H. Briand,[58] J. Chauveau,[58] P. David,[58]

L. Del Buono,[58] Ch. de la Vaissière,[58] O. Hamon,[58] B. L. Hartfiel,[58] Ph. Leruste,[58] J. Malclès,[58] J. Ocariz,[58] L. Roos,[58] G. Therin,[58] L. Gladney,[59] M. Biasini,[60] R. Covarelli,[60] C. Angelini,[61] G. Batignani,[61] S. Bettarini,[61] F. Bucci,[61] G. Calderini,[61] M. Carpinelli,[61] R. Cenci,[61] F. Forti,[61] M. A. Giorgi,[61] A. Lusiani,[61] G. Marchiori,[61] M. A. Mazur,[61] M. Morganti,[61] N. Neri,[61] E. Paoloni,[61] G. Rizzo,[61] J. J. Walsh,[61] M. Haire,[62] D. Judd,[62] D. E. Wagoner,[62] J. Biesiada,[63] N. Danielson,[63] P. Elmer,[63] Y. P. Lau,[63] C. Lu,[63] J. Olsen,[63] A. J. S. Smith,[63] A. V. Telnov,[63] F. Bellini,[64] G. Cavoto,[64] A. D'Orazio,[64] D. del Re,[64] E. Di Marco,[64] R. Faccini,[64] F. Ferrarotto,[64] F. Ferroni,[64] M. Gaspero,[64] L. Li Gioi,[64] M. A. Mazzoni,[64] S. Morganti,[64] G. Piredda,[64] F. Polci,[64] F. Safai Tehrani,[64] C. Voena,[64] M. Ebert,[65] H. Schröder,[65] R. Waldi,[65] T. Adye,[66] N. De Groot,[66] B. Franek,[66] E. O. Olaiya,[66] F. F. Wilson,[66] R. Aleksan,[67] S. Emery,[67] A. Gaidot,[67] S. F. Ganzhur,[67] G. Hamel de Monchenault,[67] W. Kozanecki,[67] M. Legendre,[67] G. Vasseur,[67] Ch. Yèche,[67] M. Zito,[67] X. R. Chen,[68] H. Liu,[68] W. Park,[68] M. V. Purohit,[68] J. R. Wilson,[68] M. T. Allen,[69] D. Aston,[69] R. Bartoldus,[69] P. Bechtle,[69] N. Berger,[69] R. Claus,[69] J. P. Coleman,[69] M. R. Convery,[69] M. Cristinziani,[69] J. C. Dingfelder,[69] J. Dorfan,[69] G. P. Dubois-Felsmann,[69] D. Dujmic,[69] W. Dunwoodie,[69] R. C. Field,[69] T. Glanzman,[69] S. J. Gowdy,[69] M. T. Graham,[69] P. Grenier,[69] V. Halyo,[69] C. Hast,[69] T. Hryn'ova,[69] W. R. Innes,[69] M. H. Kelsey,[69] P. Kim,[69] D. W. G. S. Leith,[69] S. Li,[69] S. Luitz,[69] V. Luth,[69] H. L. Lynch,[69] D. B. MacFarlane,[69] H. Marsiske,[69] R. Messner,[69] D. R. Muller,[69] C. P. O'Grady,[69] V. E. Ozcan,[69] A. Perazzo,[69] M. Perl,[69] T. Pulliam,[69] B. N. Ratcliff,[69] A. Roodman,[69] A. A. Salnikov,[69] R. H. Schindler,[69] J. Schwiening,[69] A. Snyder,[69] J. Stelzer,[69] D. Su,[69] M. K. Sullivan,[69] K. Suzuki,[69] S. K. Swain,[69] J. M. Thompson,[69] J. Va'vra,[69] N. van Bakel,[69] M. Weaver,[69] A. J. R. Weinstein,[69] W. J. Wisniewski,[69] M. Wittgen,[69] D. H. Wright,[69] A. K. Yarritu,[69] K. Yi,[69] C. C. Young,[69] P. R. Burchat,[70] A. J. Edwards,[70] S. A. Majewski,[70] B. A. Petersen,[70] C. Roat,[70] L. Wilden,[70] S. Ahmed,[71] M. S. Alam,[71] R. Bula,[71] J. A. Ernst,[71] V. Jain,[71] B. Pan,[71] M. A. Saeed,[71] F. R. Wappler,[71] S. B. Zain,[71] W. Bugg,[72] M. Krishnamurthy,[72] S. M. Spanier,[72] R. Eckmann,[73] J. L. Ritchie,[73] A. Satpathy,[73] C. J. Schilling,[73] R. F. Schwitters,[73] J. M. Izen,[74] X. C. Lou,[74] S. Ye,[74] F. Bianchi,[75] F. Gallo,[75] D. Gamba,[75] M. Bomben,[76] L. Bosisio,[76] C. Cartaro,[76] F. Cossutti,[76] G. Della Ricca,[76] S. Dittongo,[76] L. Lanceri,[76] L. Vitale,[76] V. Azzolini,[77] N. Lopez-March,[77] F. Martinez-Vidal,[77] Sw. Banerjee,[78] B. Bhuyan,[78] C. M. Brown,[78] D. Fortin,[78] K. Hamano,[78] R. Kowalewski,[78] I. M. Nugent,[78] J. M. Roney,[78] R. J. Sobie,[78] J. J. Back,[79] P. F. Harrison,[79] T. E. Latham,[79] G. B. Mohanty,[79] M. Pappagallo,[79] H. R. Band,[80] X. Chen,[80] B. Cheng,[80] S. Dasu,[80] M. Datta,[80] K. T. Flood,[80] J. J. Hollar,[80] P. E. Kutter,[80] B. Mellado,[80] A. Mihalyi,[80] Y. Pan,[80] M. Pierini,[80] R. Prepost,[80] S. L. Wu,[80] Z. Yu,[80] and H. Neal[81]

(*BABAR* Collaboration)

[1]*Laboratoire de Physique des Particules, IN2P3/CNRS et Université de Savoie, F-74941 Annecy-Le-Vieux, France*
[2]*Universitat de Barcelona, Facultat de Fisica, Departament ECM, E-08028 Barcelona, Spain*
[3]*Università di Bari, Dipartimento di Fisica and INFN, I-70126 Bari, Italy*
[4]*Institute of High Energy Physics, Beijing 100039, China*
[5]*University of Bergen, Institute of Physics, N-5007 Bergen, Norway*
[6]*Lawrence Berkeley National Laboratory and University of California, Berkeley, California 94720, USA*
[7]*University of Birmingham, Birmingham, B15 2TT, United Kingdom*
[8]*Ruhr Universität Bochum, Institut für Experimentalphysik 1, D-44780 Bochum, Germany*
[9]*University of Bristol, Bristol BS8 1TL, United Kingdom*
[10]*University of British Columbia, Vancouver, British Columbia, Canada V6T 1Z1*
[11]*Brunel University, Uxbridge, Middlesex UB8 3PH, United Kingdom*
[12]*Budker Institute of Nuclear Physics, Novosibirsk 630090, Russia*
[13]*University of California at Irvine, Irvine, California 92697, USA*
[14]*University of California at Los Angeles, Los Angeles, California 90024, USA*
[15]*University of California at Riverside, Riverside, California 92521, USA*
[16]*University of California at San Diego, La Jolla, California 92093, USA*
[17]*University of California at Santa Barbara, Santa Barbara, California 93106, USA*
[18]*University of California at Santa Cruz, Institute for Particle Physics, Santa Cruz, California 95064, USA*
[19]*California Institute of Technology, Pasadena, California 91125, USA*
[20]*University of Cincinnati, Cincinnati, Ohio 45221, USA*
[21]*University of Colorado, Boulder, Colorado 80309, USA*
[22]*Colorado State University, Fort Collins, Colorado 80523, USA*
[23]*Universität Dortmund, Institut für Physik, D-44221 Dortmund, Germany*
[24]*Technische Universität Dresden, Institut für Kern- und Teilchenphysik, D-01062 Dresden, Germany*
[25]*Laboratoire Leprince-Ringuet, CNRS/IN2P3, Ecole Polytechnique, F-91128 Palaiseau, France*
[26]*University of Edinburgh, Edinburgh EH9 3JZ, United Kingdom*

[27]*Università di Ferrara, Dipartimento di Fisica and INFN, I-44100 Ferrara, Italy*
[28]*Laboratori Nazionali di Frascati dell'INFN, I-00044 Frascati, Italy*
[29]*Università di Genova, Dipartimento di Fisica and INFN, I-16146 Genova, Italy*
[30]*Harvard University, Cambridge, Massachusetts 02138, USA*
[31]*Universität Heidelberg, Physikalisches Institut, Philosophenweg 12, D-69120 Heidelberg, Germany*
[32]*Imperial College London, London, SW7 2AZ, United Kingdom*
[33]*University of Iowa, Iowa City, Iowa 52242, USA*
[34]*Iowa State University, Ames, Iowa 50011-3160, USA*
[35]*Johns Hopkins University, Baltimore, Maryland 21218, USA*
[36]*Universität Karlsruhe, Institut für Experimentelle Kernphysik, D-76021 Karlsruhe, Germany*
[37]*Laboratoire de l'Accélérateur Linéaire, IN2P3/CNRS et Université Paris-Sud 11, Centre Scientifique d'Orsay, B.P. 34, F-91898 ORSAY Cedex, France*
[38]*Lawrence Livermore National Laboratory, Livermore, California 94550, USA*
[39]*University of Liverpool, Liverpool L69 7ZE, United Kingdom*
[40]*Queen Mary, University of London, E1 4NS, United Kingdom*
[41]*University of London, Royal Holloway and Bedford New College, Egham, Surrey TW20 0EX, United Kingdom*
[42]*University of Louisville, Louisville, Kentucky 40292, USA*
[43]*University of Manchester, Manchester M13 9PL, United Kingdom*
[44]*University of Maryland, College Park, Maryland 20742, USA*
[45]*University of Massachusetts, Amherst, Massachusetts 01003, USA*
[46]*Massachusetts Institute of Technology, Laboratory for Nuclear Science, Cambridge, Massachusetts 02139, USA*
[47]*McGill University, Montréal, Québec, Canada H3A 2T8*
[48]*Università di Milano, Dipartimento di Fisica and INFN, I-20133 Milano, Italy*
[49]*University of Mississippi, University, Mississippi 38677, USA*
[50]*Université de Montréal, Physique des Particules, Montréal, Québec, Canada H3C 3J7*
[51]*Mount Holyoke College, South Hadley, Massachusetts 01075, USA*
[52]*Università di Napoli Federico II, Dipartimento di Scienze Fisiche and INFN, I-80126, Napoli, Italy*
[53]*NIKHEF, National Institute for Nuclear Physics and High Energy Physics, NL-1009 DB Amsterdam, The Netherlands*
[54]*University of Notre Dame, Notre Dame, Indiana 46556, USA*
[55]*Ohio State University, Columbus, Ohio 43210, USA*
[56]*University of Oregon, Eugene, Oregon 97403, USA*
[57]*Università di Padova, Dipartimento di Fisica and INFN, I-35131 Padova, Italy*
[58]*Laboratoire de Physique Nucléaire et de Hautes Energies, IN2P3/CNRS, Université Pierre et Marie Curie-Paris6, Université Denis Diderot-Paris7, F-75252 Paris, France*
[59]*University of Pennsylvania, Philadelphia, Pennsylvania 19104, USA*
[60]*Università di Perugia, Dipartimento di Fisica and INFN, I-06100 Perugia, Italy*
[61]*Università di Pisa, Dipartimento di Fisica, Scuola Normale Superiore and INFN, I-56127 Pisa, Italy*
[62]*Prairie View A&M University, Prairie View, Texas 77446, USA*
[63]*Princeton University, Princeton, New Jersey 08544, USA*
[64]*Università di Roma La Sapienza, Dipartimento di Fisica and INFN, I-00185 Roma, Italy*
[65]*Universität Rostock, D-18051 Rostock, Germany*
[66]*Rutherford Appleton Laboratory, Chilton, Didcot, Oxon, OX11 0QX, United Kingdom*
[67]*DSM/Dapnia, CEA/Saclay, F-91191 Gif-sur-Yvette, France*
[68]*University of South Carolina, Columbia, South Carolina 29208, USA*
[69]*Stanford Linear Accelerator Center, Stanford, California 94309, USA*
[70]*Stanford University, Stanford, California 94305-4060, USA*
[71]*State University of New York, Albany, New York 12222, USA*
[72]*University of Tennessee, Knoxville, Tennessee 37996, USA*
[73]*University of Texas at Austin, Austin, Texas 78712, USA*
[74]*University of Texas at Dallas, Richardson, Texas 75083, USA*
[75]*Università di Torino, Dipartimento di Fisica Sperimentale and INFN, I-10125 Torino, Italy*
[76]*Università di Trieste, Dipartimento di Fisica and INFN, I-34127 Trieste, Italy*
[77]*IFIC, Universitat de Valencia-CSIC, E-46071 Valencia, Spain*
[78]*University of Victoria, Victoria, British Columbia, Canada V8W 3P6*
[79]*Department of Physics, University of Warwick, Coventry CV4 7AL, United Kingdom*
[80]*University of Wisconsin, Madison, Wisconsin 53706, USA*
[81]*Yale University, New Haven, Connecticut 06511, USA*

[*]Also with Università di Perugia, Dipartimento di Fisica, Perugia, Italy
[†]Also with Università della Basilicata, Potenza, Italy

(Received 5 September 2006; published 9 January 2007)

We present measurements of the total production rates and momentum distributions of the charmed baryon Λ_c^+ in $e^+e^- \to$ hadrons at a center-of-mass energy of 10.54 GeV and in $\Upsilon(4S)$ decays. In hadronic events at 10.54 GeV, charmed hadrons are almost exclusively leading particles in $e^+e^- \to c\bar{c}$ events, allowing direct studies of c-quark fragmentation. We measure a momentum distribution for Λ_c^+ baryons that differs significantly from those measured previously for charmed mesons. Comparing with a number of models, we find none that can describe the distribution completely. We measure an average scaled momentum of $\langle x_p \rangle = 0.574 \pm 0.009$ and a total rate of $N_{\Lambda_c}^{q\bar{q}} = 0.057 \pm 0.002(\text{exp.}) \pm 0.015(\text{BF})$ Λ_c^+ per hadronic event, where the experimental error is much smaller than that due to the branching fraction into the reconstructed decay mode, $pK^-\pi^+$. In $\Upsilon(4S)$ decays we measure a total rate of $N_{\Lambda_c}^{\Upsilon} = 0.091 \pm 0.006(\text{exp.}) \pm 0.024(\text{BF})$ per $\Upsilon(4S)$ decay, and find a much softer momentum distribution than expected from B decays into a Λ_c^+ plus an antinucleon and one to three pions.

DOI: 10.1103/PhysRevD.75.012003 PACS numbers: 13.66.Bc, 13.20.He, 13.60.Rj

I. INTRODUCTION

The production properties of charmed baryons in e^+e^- annihilations into $c\bar{c}$ and in decays of bottom (b) hadrons probe different aspects of strong interaction physics. Experiments running at and below the $\Upsilon(4S)$ resonance are uniquely positioned to explore each of these processes in detail. The CLEO experiment has made precise studies of charmed mesons in this way [1], and the larger data samples available at the B factories have allowed improved studies of charmed mesons [2] and the first precise studies of charmed baryons [2,3].

Heavy hadrons (H) produced in e^+e^- annihilations provide a laboratory for the study of heavy-quark ($Q = c, b$) jet fragmentation, in terms of both the relative production rates of hadrons with different quantum numbers and their associated spectra. The latter can be characterized in terms of a scaled energy or momentum, such as $x_p \equiv p_H^*/p_{\text{max}}^*$, where p_H^* is the hadron momentum in the e^+e^- center-of-mass (c.m.) frame and $p_{\text{max}}^* = \sqrt{s/4 - m_H^2}$ is the maximum momentum available to a particle of mass m_H at a c.m. energy of $\sqrt{s}$. For $\sqrt{s} \gg 2m_H$ it has been observed [4] that the x_p distributions $P(x_p)$ for heavy hadrons peak at relatively high values, and that very few b hadrons are produced apart from those containing initial b quarks, so that one can probe leading b-hadron production directly. This is also the case for charmed (c) hadrons when $\sqrt{s} < 2m_B$, where m_B is the mass of the lightest b meson, but above $B\bar{B}$ threshold a large fraction of the c hadrons are b-hadron decay products.

Since the hadronization process is intrinsically nonperturbative, $P(x_p)$ cannot be calculated using perturbative quantum chromodynamics (QCD). However, a high quark mass provides a convenient cutoff point and the distribution of the scaled momentum of the heavy quark before hadronization, $x_Q \equiv 2p_Q^*/\sqrt{s}$, can be calculated [5–8]. The observable $P(x_p)$ is thought to be related by a simple convolution or hadronization model. Several phenomenological models of heavy-quark fragmentation have been proposed [9–12]. Predictions depend on the mass of the heavy quark, with $P(x_p)$ being much harder for b hadrons than c hadrons, and in some cases on the mass and quantum numbers of H. Hadrons containing the same heavy quark type are generally predicted to have quite similar $P(x_p)$, although differences between mesons and baryons have been suggested [13,14]. Measurements of $P(x_p)$ serve to constrain perturbative QCD and these model predictions. Furthermore, measurements for a given c or b hadron at different $\sqrt{s}$ can test QCD evolution, and comparisons of c- and b-hadron distributions can test heavy-quark symmetry [15].

The inclusive b-hadron scaled energy distribution and its average value of 0.71 have been measured precisely [16] by experiments at the Z^0, using partial reconstruction techniques. However, these techniques do not distinguish the different types of b hadrons. The relative production of B_u^-, B_d^0, B_s^0, excited b mesons, and b baryons have been measured [4,17], but with limited precision and no sensitivity to differences in their x_p distributions. Several c mesons have been studied at the Z^0 [18], but it is difficult to disentangle the leading charm and b-decay contributions and neither component is measured precisely. Recent measurements below $B\bar{B}$ threshold [1,2] have good precision over the full x_p range and show substantial differences between the pseudoscalar D and vector D^* meson states. $P(x_p)$ has been measured below $B\bar{B}$ threshold for two charmed baryons, Λ_c^+ by CLEO [19] and Belle [2], and Ξ_c^0 by *BABAR* [3], but with limited statistics, especially at low x_p. In this article we use the excellent particle identification of the *BABAR* experiment to isolate Λ_c^+ baryons (the inclusion of charge conjugate states is implied throughout) in a large data sample collected below $B\bar{B}$ threshold, at $\sqrt{s} = 10.54$ GeV. We measure $P(x_p)$ precisely, and compare our results with available predictions and previous measurements of heavy hadrons.

The large b-hadron masses allow many hadronic decay modes, a small fraction of which have been studied in detail. The $\Upsilon(4S)$ resonance provides a unique laboratory, in which no b baryons are produced and decays of mesons into baryons can be studied directly. Many c baryons have

been observed in inclusive $\Upsilon(4S)$ decays [4] and the low rate of associated leptons and high rate of "wrong-sign" Λ_c^+ [20] suggest interesting dynamics. However only a few exclusive decays with c baryons have been observed [21–23]. Again, momentum distributions have been measured only for the Λ_c^+ [2,24] and Ξ_c^0 [3] with limited precision. Here we use data collected on the $\Upsilon(4S)$ resonance ($\sqrt{s} =$ 10.58 GeV) and subtract the $e^+e^- \to c\bar{c}$ contribution measured at $\sqrt{s} = 10.54$ GeV to make a precise measurement of the Λ_c^+ momentum distribution in B meson decays, which we compare with a number of possible models.

In Sec. II, we describe the *BABAR* detector, in particular, the particle identification capabilities essential to these measurements. In Secs. III and IV, we discuss the selection of Λ_c^+ candidates and the measurement of their x_p distributions, respectively. We interpret the results for $e^+e^- \to q\bar{q}$ events and $\Upsilon(4S)$ decays in Secs. V and VI, respectively, and summarize in Sec. VII.

II. APPARATUS AND EVENT SELECTION

In this analysis, we use data samples corresponding to 9.5 fb^{-1} of integrated luminosity at $\sqrt{s} = 10.54$ GeV and 81 fb^{-1} on the $\Upsilon(4S)$ resonance, $\sqrt{s} = 10.58$ GeV. The *BABAR* detector is located at the PEP-II asymmetric-energy e^+e^- collider at the Stanford Linear Accelerator Center and is described in detail in Ref. [25]. We use charged tracks measured in the five-layer, double sided silicon vertex tracker (SVT) and the 40-layer drift chamber (DCH). In a 1.5 T axial magnetic field, they provide a combined resolution on the momentum p_T transverse to the beam axis of $[\sigma(p_T)/p_T]^2 = [0.0013p_T]^2 + 0.0045^2$, where p_T is measured in GeV/c.

Charged particle identification uses a combination of the energy loss (dE/dx) measured in the DCH, and information from the detector of internally reflected Cherenkov light (DIRC). The DCH gas is helium:isobutane 80:20 and a typical cell size is 18 mm. A truncated mean algorithm gives a dE/dx value for each track with an average resolution of 7.5%, from which we calculate a set of five relative likelihoods $L_i^{\rm DCH}$ for the particle hypotheses $i = e$, μ, π, K, and p. Differences between the log-likelihoods $l_{ij}^{\rm DCH} = \ln(L_i^{\rm DCH}) - \ln(L_j^{\rm DCH})$ are used as input to the particle identification algorithm.

The DIRC comprises 144 fused silica bars that guide Cherenkov photons to an expansion volume filled with water and equipped with 10 752 photomultiplier tubes. The fused silica refractive index is 1.473, corresponding to Cherenkov thresholds of 128, 458, and 867 MeV/c for pions, kaons, and protons, respectively. A particle well above threshold yields 20–75 measured photons, each with a Cherenkov angle resolution of about 10 mrad. A global likelihood algorithm considers all the reconstructed charged tracks and detected photons in each event and assigns each track a set of likelihoods $L_i^{\rm DIRC}$.

The DCH provides excellent K-π and p-K separation for momenta in the laboratory frame below 0.5 and 0.9 GeV/c, respectively. The DIRC provides very good separation for momenta above 1.0 and 1.5 GeV/c, respectively. In both detectors the separation power is lower for tracks with polar angles near 90° in the laboratory than for more forward or backward tracks. To minimize the systematic errors in this analysis, the identification efficiencies must not vary rapidly as a function of momentum or polar angle. We have therefore developed an algorithm that uses linear combinations of $l_{ij}^{\rm DCH}$ and $l_{ij}^{\rm DIRC}$ chosen to minimize such variations. It is described in detail in Ref. [26] and its performance for tracks used in this analysis is shown as a function of momentum in Fig. 1. The identification efficiencies are better than 99% at low momenta and above 90% for the majority of Λ_c^+ decay products. They are seen to vary smoothly with momentum, and are almost inde-

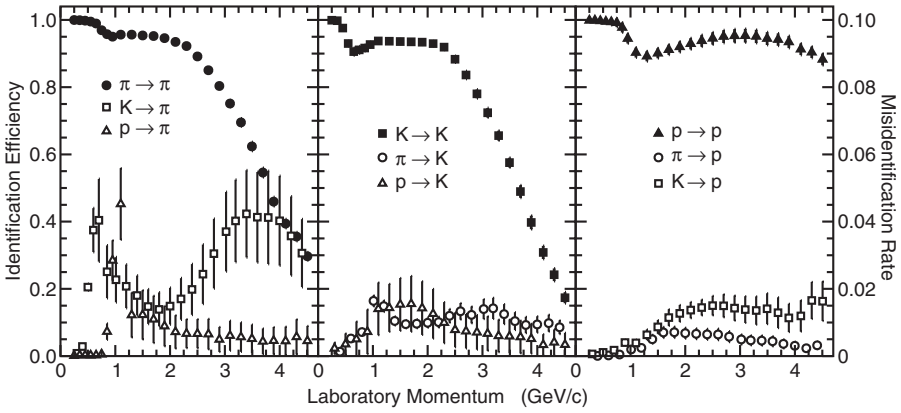

FIG. 1. Efficiencies for identifying (solid symbols, left-hand vertical scale) or misidentifying (open symbols, right-hand scale) selected pions (circles), kaons (squares), and protons (triangles) within the DIRC acceptance as pions (left), kaons (center), or protons (right). They are extracted from control samples in the data as smooth functions of momentum and polar angle, and shown in momentum bins averaged over the polar angle range used. The error bars indicate the average uncertainty due to control sample statistics.

pendent of polar angle except near 0.8 GeV/c (1.2 GeV/c) for pions and kaons (protons), where they are as much as 10% lower for central tracks than for forward/backward tracks. The misidentification rates depend strongly on polar angle in the momentum regions 0.6–0.8, 1.1–1.3, and 2.5–3.5 GeV/c. They are below 5% everywhere except that the rate for kaons (protons) to be misidentified as pions reaches 11% at 0.7(1.2) GeV/c for the most central tracks. These rates have negligible effects on the results. About 16% of the selected tracks have good DCH information but are outside the DIRC fiducial acceptance. These can be identified with essentially the same efficiencies as in Fig. 1 for pion and kaon (proton) momenta below 0.6(0.9) GeV/c.

The event selection requires three or more charged tracks in the event, which retains any $e^+e^- \to q\bar{q}$ event or $\Upsilon(4S)$ decay containing a reconstructable $\Lambda_c^+ \to pK^-\pi^+$ decay and suppresses beam-related backgrounds. We evaluate its performance using a number of simulations, each consisting of a generator for a certain type of event combined with a detailed simulation of the *BABAR* detector [27]. For $e^+e^- \to q\bar{q}$ events we use the JETSET [28] generator and for $\Upsilon(4S)$ events we use our own generator, EVTGEN [29], in which the $\Upsilon(4S)$ decays into a $B\bar{B}$ pair, then the B and $\bar{B}$ decay using a combination of measured exclusive and semiexclusive modes, and a $b \to cW^-$ model tuned to the world's inclusive data. We study large samples of simulated two-photon, τ-pair, and radiative e- and μ-pair events, and find their contributions to both signal and background to be negligible.

III. $\Lambda_c^+ \to pK^-\pi^+$ SELECTION

We construct Λ_c^+ candidates from charged tracks that are consistent with originating at the e^+e^- interaction point and have good tracking and particle identification information. Each track must have: (i) at least 20 measured coordinates in the DCH; (ii) at least 5 coordinates in the SVT, including at least three in the direction along the e^- beam; (iii) a distance of closest approach to the beam axis below 1 mm; and (iv) a z-coordinate at this point within 10 cm of the nominal interaction point. These criteria ensure good quality information from the DCH and a well-measured entrance angle into the DIRC. If the extrapolated trajectory intersects a DIRC bar then the track is accepted if it is identified as a pion, kaon, or proton by the combined DCH and DIRC algorithm. If not, then it is accepted if it is identified as a proton (pion or kaon) using DCH information only and has a momentum below 1.2(0.6) GeV/c.

We consider a combination of three charged tracks as a Λ_c^+ candidate if the total charge is $+1$, one of the positively charged tracks is identified as a proton and the other as a pion, and the negatively charged track is identified as a kaon. With the appropriate particle type assigned to each track, we correct their measured momenta for energy loss and calculate their combined four momentum from their momenta at their points of closest approach to the beam axis. The distributions of invariant mass for the candidates in the on- and off-resonance data are shown in Fig. 2; Λ_c^+ signals of about 137 000 and 13 000 decays, respectively, are visible over nearly uniform backgrounds.

The Λ_c^+ reconstruction efficiency depends primarily on the momenta p and polar angles θ of the daughter tracks in the laboratory frame. To reduce systematic uncertainty, we apply an efficiency correction to each candidate before boosting it into the e^+e^- c.m. frame. The efficiencies for reconstructing and identifying tracks from pions, kaons, and protons are determined from large control samples in the data as two-dimensional functions of (p, θ). We use these efficiencies in dedicated simulations of $q\bar{q}$ and $\Upsilon(4S)$ events containing a Λ_c^+ baryon that is decayed into $pK^-\pi^+$. From these we calculate the Λ_c^+ selection efficiency ε as a smooth two-dimensional function of (p, θ) of the Λ_c^+. We check that the efficiency does not depend on other track or event variables, in particular, that it is the same in simulated $q\bar{q}$ and $\Upsilon(4S)$ events for given values of (p, θ). The resolutions on the Λ_c^+ momentum and polar angle are much smaller than the bin sizes used below, so we include resolution effects by defining the efficiency as the number of Λ_c^+ reconstructed within a given (p, θ) range divided by the number generated in that range, using ranges smaller than the relevant bin sizes. We test the efficiency using a number of simulations, and find biases to be below 1%.

The efficiency varies rapidly near the edges of the detector acceptance and at very low momenta in the laboratory. We make the tight fiducial requirement that θ^*, the polar angle of the Λ_c^+ candidate in the e^+e^- c.m. frame, satisfy $-0.7 < \cos\theta^* < 0.2$, which reduces model dependence and rejects all candidates in regions with efficiency

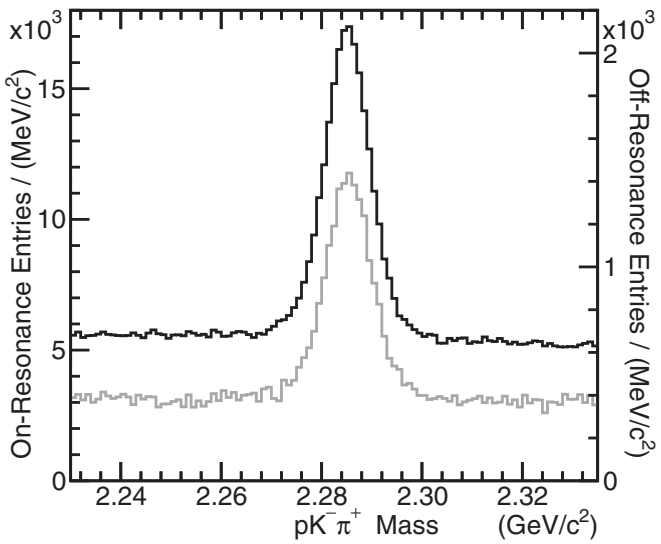

FIG. 2. Invariant mass distributions for Λ_c^+ candidates in the on-(black) and off-resonance (gray) data.

below about 5%, including those with a total laboratory momentum below about 0.7 GeV/c. A feature of the boosted c.m. system is that true Λ_c^+ baryons with low c.m. momentum p^* are boosted forward and often have all three tracks in the detector acceptance, giving efficient access to the full p^* range.

We define A_k as the fraction of the Λ_c^+ in events of type k produced within our fiducial range $-0.7 < \cos\theta^* < 0.2$. In $\Upsilon(4S) \to B\bar{B} \to \Lambda_c^+ X$ decays, the true $\cos\theta^*$ distribution is uniform and $A_\Upsilon = 0.45$. In $c\bar{c}$ events the angular distribution of the initial c-quark follows $1 + \cos^2\theta^*$, and we use the JETSET simulation to calculate the distribution for Λ_c^+ after QCD radiation and hadronization. Soft Λ_c^+ are produced predominantly in events with hard gluon radiation, which flattens the distribution considerably. The resulting value of $A_{c\bar{c}}$ is 0.46 at $p^* = 0$, and falls with increasing p^* toward an asymptotic value of 0.38.

We bin candidates according to their reconstructed values of $x_p = p^*/p^*_{\rm max}$, where $p^*_{\rm max}$ is calculated for each event from its c.m. energy and the nominal Λ_c^+ mass [4]. Figure 3 shows the average value in each x_p bin of the product $A_{c\bar{c}}(p^*) \cdot \varepsilon(p, \theta)$ for selected candidates in the off-resonance data. It ranges from 8% at low x_p to 19% at high x_p. The error bars represent the statistical uncertainty on the efficiency calculation. The corresponding quantity for Λ_c^+ from $\Upsilon(4S)$ decays, $\langle A_\Upsilon \cdot \varepsilon(p, \theta)\rangle$, is slightly higher at low x_p due to a small dependence of ε on θ, and rises faster with increasing x_p since A_Υ is constant, whereas $A_{c\bar{c}}$ decreases. We give each candidate a weight equal to the inverse of either $A_{c\bar{c}} \cdot \varepsilon$ or $A_\Upsilon \cdot \varepsilon$, as specified below. The RMS deviation of the weights in each bin is always much smaller than the average value.

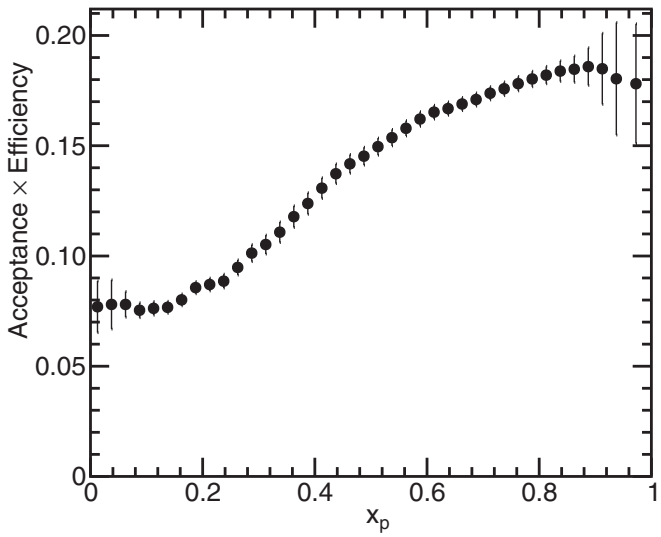

FIG. 3. Average value of $A_{c\bar{c}} \cdot \varepsilon$, the $\Lambda_c^+ \to pK^-\pi^+$ acceptance times reconstruction efficiency, for candidates in the off-resonance data in bins of scaled momentum x_p. The error bars represent the average statistical uncertainty.

IV. SIGNAL EXTRACTION

To estimate the number of $\Lambda_c^+ \to pK^-\pi^+$ decays in each x_p bin in the data, we fit the weighted invariant mass distribution with a function comprising signal and background components. Based on the simulated mass distributions, we describe the signal with a sum of two Gaussian functions of common mean value, one of which has 1.5 times the width and one quarter of the area of the other, and correct for a 1.3% residual bias in the fitted area. We check the simulated bias by comparing with a single Gaussian signal function. The change in the yields is 1.2% in both data and simulation.

The simulation predicts a nearly uniform background over the $pK^-\pi^+$ mass range shown in Fig. 2. We search for reflections in the data by changing the particle mass assignments. We observe signals for $D^+ \to K^-\pi^+\pi^+$ (π^+ misidentified as p) and $D_s^+ \to K^-K^+\pi^+$ (K^+ misidentified as p) at very low levels consistent with the predictions of our detector simulation, but no unexpected structure. From these studies we calculate that reflections known to give broad structures in the vicinity of the Λ_c^+ peak, such as $D^{*+} \to K^-\pi^+\pi^+$ (π^+ misidentified as p) contribute a number of entries in each bin much smaller than the statistical fluctuations. We also study processes such as $\Sigma_c^{++} \to \Lambda_c^+\pi^+$, with the wrong π^+ included in the Λ_c^+ candidate, and find their contributions to be negligible. In each x_p bin, a linear function describes the mass distribution in the data over a wide range away from the Λ_c^+ peak region, so we use a linear background function and perform fits over the range 2235–2335 MeV/c^2.

We first fit the full data sample in each x_p bin in order to study mass resolution and bias. These fits yield Λ_c^+ mass values that vary slightly with x_p in a manner consistent with the simulation and our recent measurement of the Λ_c^+ mass [30]. The fitted mass resolutions (RMS width of the signal function) are shown as a function of x_p in Fig. 4. The simulation is consistent with the data at low x_p, and is slightly optimistic at high x_p. The effect of this difference on the efficiency estimate is negligible.

Next we fix the mean and width of the signal function in each x_p bin to values from linear parametrizations, and perform fits to the on- and off-resonance data separately. Dividing the signal yields by the integrated luminosity, bin width, and branching fraction $\mathcal{B}_{pK^-\pi^+} \equiv \mathcal{B}(\Lambda_c^+ \to pK^-\pi^+) = 5.0 \pm 1.3\%$ [4] gives the differential production cross sections shown in Fig. 5 with statistical errors only. We use the $e^+e^- \to c\bar{c}$ acceptance factor $A_{c\bar{c}}$ for the off-resonance data and, for purposes of this comparison, an average value of A in each bin weighted by the relative production rates measured below (see Tables I and V) for the on-resonance data. There are two broad peaks in the on-resonance cross section, corresponding to the contributions from $\Upsilon(4S)$ decays at low x_p and from $e^+e^- \to c\bar{c}$ events at high x_p. For $x_p > 0.47$, the kinematic limit for a B decay

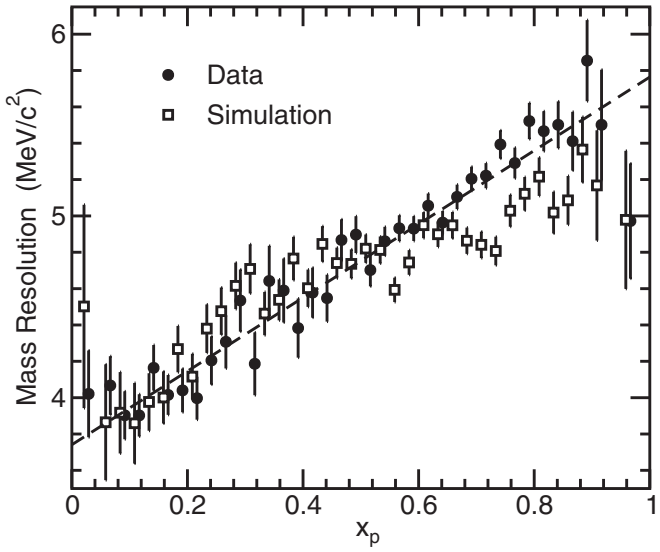

FIG. 4. RMS width of the fitted Λ_c^+ signal function in the data (circles) and simulation (squares) as a function of x_p. The line represents a linear parametrization of the data.

including a Λ_c^+ and an antiproton, the two cross sections are consistent, indicating no visible contribution from $\Upsilon(4S)$ events.

We extract the cross section for $\Upsilon(4S)$ decays by repeating the analysis using A_Υ for both data sets. In each x_p bin we then subtract the off-resonance cross section, scaled down by 0.8% to account for the dependence of the cross section on the c.m. energy, from the on-resonance cross section. We divide the off-resonance and $\Upsilon(4S)$ cross sections by the $e^+e^- \to$ hadrons and effective $e^+e^- \to \Upsilon(4S)$ cross sections, respectively, to yield the differential

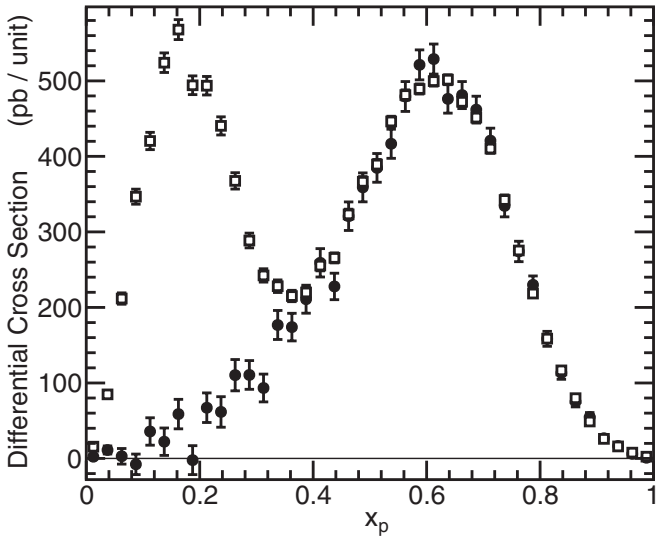

FIG. 5. Differential cross sections for $\Lambda_c^+ + \bar{\Lambda}_c^-$ production in the off-(circles) and on-resonance (open squares) data as functions of x_p. The errors are statistical only.

production rates per event discussed in the following sections.

We consider several sources of systematic uncertainty. We propagate the uncertainties on the measured track finding and particle identification efficiencies by recalculating $\varepsilon(p, \theta)$ with all efficiencies of a given type varied simultaneously and repeating the fits. Tracking gives an uncertainty of 2.5% and the particle identification contributions total 1.5%–2.1%, depending on x_p. We obtain a 0.9% uncertainty due to the resonant substructure of the $\Lambda_c^+ \to pK^-\pi^+$ decay similarly. The uncertainty on our integrated luminosity is 1.0%. Simulation statistics contribute 2%–4% where the rate is significantly nonzero. We check the fitting procedure by floating the signal mean and/or width, fixing them to nominal or fitted values, using a single Gaussian signal function, using a quadratic background function, and varying the bin size. All changes in the signal yields are less than the corresponding statistical errors, and we take the largest change in each x_p bin as a systematic uncertainty. Each simulated bias is varied by $\pm 50\%$; together they contribute 0.7% to the systematic uncertainty. The imperfect x_p distribution used in the efficiency calculation can affect the result if the efficiency varies over the width of an x_p bin. We recalculate the efficiency with the input distribution shifted by plus and minus our bin width to derive a conservative limit on any such effect of 0.5%–1.9%, depending on x_p, which we take as a systematic uncertainty.

We also perform several systematic checks of the results. The cross sections measured separately for Λ_c^+ and $\bar{\Lambda}_c^-$, which have very different efficiencies at low laboratory momentum, are consistent. Cross sections measured in six different regions of $\cos\theta^*$ are consistent with each other. Because of the boosted c.m. system, these would be affected differently by any deficiency in the detector simulation, especially at low x_p. They also have very different $A_{c\bar{c}}$ values, and these studies indicate that the uncertainties due to both the production angle model in $c\bar{c}$ events and the value of the boost are negligible.

V. RESULTS FOR $\sqrt{s} = 10.54$ GeV

A. Λ_c^+ Baryon production

The differential Λ_c^+ production rate per hadronic event $(1/N_{q\bar{q}})(dN_{\Lambda c}^{q\bar{q}}/dx_p)$ is tabulated in Table I and compared with previous charmed baryon measurements in Fig. 6. We distinguish between systematic uncertainties that affect the shape of the cross section and those that affect only its normalization. The former include both uncertainties that are uncorrelated between bins and the parts of the correlated uncertainties whose values depend on x_p. The uncertainty from the fitting procedure has negligible correlation between bins, and those from the particle identification and the shift of the simulated distribution have only very short-range correlations, so we include them in the uncorrelated

TABLE I. Λ_c^+ differential production rate per hadronic event per unit x_p at $\sqrt{s} = 10.54$ GeV. The last column includes experimental errors that are correlated between x_p values and affect the shape of the distribution. Normalization uncertainties are given only on the total.

x_p Range	$\frac{1}{N_{q\bar{q}}}\frac{dN_{\Lambda c}^{q\bar{q}}}{dx_p}$	Statistical Error	Systematic Independent	Systematic Correlated
0.000–0.025	0.0007	0.0009	0.0004	0.0001
0.025–0.050	0.0033	0.0016	0.0012	0.0002
0.050–0.075	0.0008	0.0030	0.0011	0.0001
0.075–0.100	−0.0023	0.0040	0.0013	0.0001
0.100–0.125	0.0105	0.0053	0.0020	0.0007
0.125–0.150	0.0065	0.0053	0.0041	0.0002
0.150–0.175	0.0172	0.0057	0.0024	0.0004
0.175–0.200	−0.0006	0.0056	0.0036	0.0000
0.200–0.225	0.0197	0.0057	0.0038	0.0004
0.225–0.250	0.0180	0.0059	0.0039	0.0003
0.250–0.275	0.0323	0.0061	0.0064	0.0006
0.275–0.300	0.0324	0.0056	0.0040	0.0006
0.300–0.325	0.0273	0.0054	0.0064	0.0006
0.325–0.350	0.0517	0.0056	0.0053	0.0011
0.350–0.375	0.0509	0.0053	0.0029	0.0010
0.375–0.400	0.0617	0.0054	0.0045	0.0012
0.400–0.425	0.0759	0.0055	0.0040	0.0014
0.425–0.450	0.0667	0.0051	0.0032	0.0010
0.450–0.475	0.0939	0.0055	0.0044	0.0014
0.475–0.500	0.1051	0.0056	0.0041	0.0014
0.500–0.525	0.1126	0.0056	0.0048	0.0014
0.525–0.550	0.1220	0.0056	0.0043	0.0015
0.550–0.575	0.1403	0.0058	0.0041	0.0014
0.575–0.600	0.1526	0.0058	0.0044	0.0015
0.600–0.625	0.1548	0.0058	0.0061	0.0014
0.625–0.650	0.1394	0.0055	0.0038	0.0012
0.650–0.675	0.1409	0.0052	0.0045	0.0012
0.675–0.700	0.1352	0.0052	0.0037	0.0011
0.700–0.725	0.1232	0.0049	0.0035	0.0010
0.725–0.750	0.0979	0.0043	0.0030	0.0009
0.750–0.775	0.0803	0.0040	0.0026	0.0007
0.775–0.800	0.0673	0.0034	0.0035	0.0008
0.800–0.825	0.0464	0.0029	0.0026	0.0006
0.825–0.850	0.0332	0.0025	0.0017	0.0004
0.850–0.875	0.0220	0.0020	0.0010	0.0005
0.875–0.900	0.0161	0.0017	0.0017	0.0006
0.900–0.925	0.0079	0.0013	0.0007	0.0003
0.925–0.950	0.0049	0.0012	0.0006	0.0008
0.950–0.975	0.0018	0.0006	0.0003	0.0004
0.975–1.000	0.0003	0.0001	0.0002	0.0001
Total	0.0568	0.0007	0.0006	0.0008
Norm. err.	0.0016			
BF error	0.0148			

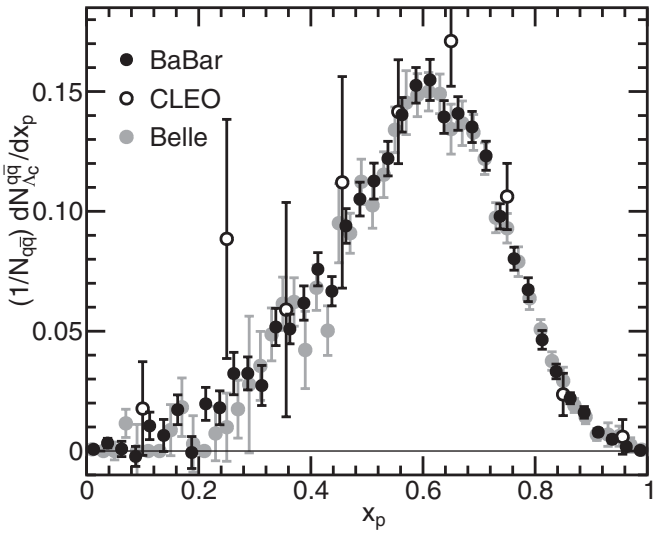

FIG. 6. Differential Λ_c^+ production rate per $e^+e^- \to q\bar{q}$ event compared with previous measurements. The error bars include statistics and those systematic errors that affect the shape. Each experiment has a normalization uncertainty of a few percent, and there is an overall 26% uncertainty due to the $\Lambda_c^+ \to pK^-\pi^+$ branching fraction.

category. We express the error matrix for the efficiency calculation as the sum of a diagonal ''uncorrelated'' matrix and a remainder matrix, in which the elements of the former are as large as possible but no correlation coefficient in the latter exceeds unity. The sum in quadrature of the uncorrelated uncertainties is listed in the ''independent'' column of Table I. It is typically 3% in the peak region, increasing to 10% where the cross section is one-third of its peak value, and becoming relatively large at the ends of the x_p range. The square roots of the diagonal elements of the remainder matrix are listed in the ''correlated'' column of Table I, and included with the independent and statistical components in the error bars in the figures.

All other uncertainties are fully correlated between bins and very nearly independent of x_p, so are considered experimental normalization uncertainties. They total 2.9%, dominated by the track-finding efficiency. There is a 26% uncertainty on $\mathcal{B}_{pK^-\pi^+}$ that also affects the normalization. The integral of the differential rate, taking the correlation in the errors into account, gives the total rate, listed at the bottom of Table I along with the normalization uncertainties. The product of the total rate per event and branching fraction of $N_{\Lambda c}^{q\bar{q}} \cdot \mathcal{B}_{pK^-\pi^+} = 2.84 \pm 0.04(\text{stat.}) \pm 0.09(\text{syst.}) \times 10^{-3}$ is consistent with, and more precise than, previous measurements. The normalization uncertainties are not included in any of the figures, and all rates shown assume the same value of $\mathcal{B}_{pK^-\pi^+}$.

Assuming the Λ_c^+ are produced predominantly in $e^+e^- \to c\bar{c}$ events, the total rate corresponds to a rate of $N_{\Lambda c}^c = 0.071 \pm 0.003(\text{exp.}) \pm 0.018$ (BF) Λ_c^+ per c-quark jet. Roughly 10% of the particles in high-energy jets have generally been observed to be baryons [4], and our measurement is consistent with 10% of c jets producing a c baryon, with a large fraction of these decaying via a Λ_c^+. All known nonstrange charmed baryons decay predomi-

nantly through a Λ_c^+, whereas no Ω_c states and only the heaviest observed Ξ_c states [31] are known to decay through a Λ_c^+, so that 70%–85% of inclusive charmed baryons would be expected to decay through a Λ_c^+ in current hadronization models.

The shape of the differential production rate is consistent with previous results and measured more precisely. It is quite hard, as expected, peaking near $x_p = 0.6$. We normalize the rate to unit area to obtain $P(x_p)$, and compare it with previously measured distributions for Ξ_c^0 baryons and D and D^* mesons in Fig. 7. The Ξ_c^0 distribution is normalized to have the same peak height as the Λ_c^+ distribution, and, since it was measured on the $\Upsilon(4S)$ resonance, is shown only above the kinematic limit for B-meson decays. The two charmed baryons have similar distributions, with that for the heavier baryon shifted up in x_p by roughly 0.05. Although qualitatively similar, the D meson distributions show broader peaks than the baryon distributions and differ greatly in the way they fall toward zero at high x_p. The charmed baryon and meson distributions are all much softer than the inclusive B-hadron distribution at c.m. energies well above $b\bar{b}$ threshold, which peaks around $x_p = 0.75$ [16].

The average x_p value is often used in comparisons between different heavy hadrons, and the higher moments

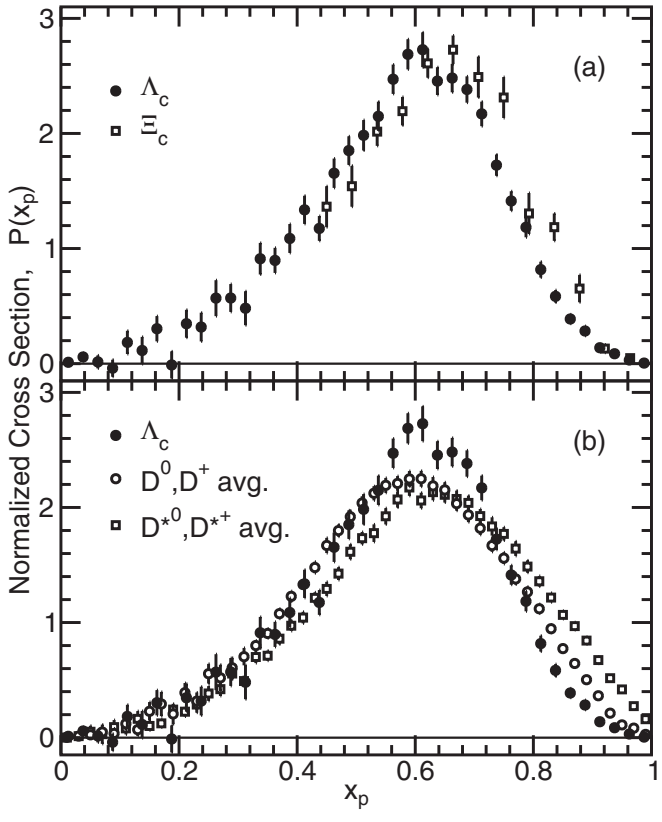

FIG. 7. x_p distribution for Λ_c^+ in $e^+e^- \to q\bar{q}$ events compared with those measured for (a) Ξ_c^0 by *BABAR* [3] and (b) charmed mesons by Belle [2].

of the distribution are of theoretical interest. In Table II we list values of the first six moments of the x_p distribution, calculated by summing over bins. They are consistent with previous measurements from Belle [2]; all are 1–2 standard deviations lower, but the moments are strongly correlated with each other. The $\langle x_p \rangle$ value of 0.574 ± 0.009 is consistent with those measured [2] for D^0 and D^+ mesons, and about 5% lower than those for D^{*0} and D^{*+} mesons.

B. Tests of *c*-quark fragmentation models

Testing models of heavy-quark fragmentation can be problematic since the predictions are usually functions of a variable z that is not accessible experimentally, such as $z_1 = (E + p_\parallel)_H/(E + p_\parallel)_Q$, $z_2 = p_{\parallel H}/p_{\parallel Q}$, or $z_3 = p_H/p_{H\,\max}(p_Q)$, where $p_\parallel$ represents a momentum projection on the flight direction of the heavy quark before it hadronizes. Monte Carlo event generators use similar internal variables, and in some cases can be made to produce events according to a given input function $f(z, \beta)$, where β represents the set of model parameters. In this way one can test the large-scale features of any model, although the detailed structure may not be reproduced exactly.

We consider the perturbative QCD calculations of Collins and Spiller (CS) [5] and Braaten *et al.* (BCFY) [7], as well as the phenomenological models of Kartvelishvili *et al.* for mesons (KLP-M) [9] and baryons (KLP-B) [13], Bowler [10], Peterson *et al.* [11], the Lund group [12], the UCLA group [14], and the HERWIG group [32]. The latter two include heavy-quark fragmentation within their own generators, and the other seven predict the functional forms listed in Table III. We implement each of these functions $f(z, \beta)$ within the JETSET generator. JETSET uses z_1 as its internal variable, but z_2 and z_3 are very similar at high x_p where we are most sensitive to the shape. All distributions are affected by JETSET's simulation of hard and soft gluon radiation.

We test each model against our measured $P(x_p)$ using a binned χ^2

$$\chi^2 = \sum_{i,j=1}^{n} (P_i^{\text{data}} - P_i^{\text{MC}}) \mathbf{V}_{i,j}^{-1} (P_j^{\text{data}} - P_j^{\text{MC}}), \qquad (1)$$

TABLE II. The first six moments of the Λ_c^+ x_p distribution in hadronic events at $\sqrt{s} = 10.54$ GeV.

			Systematic		
Moment	Value	Stat. Error	Indep.	Correl.	Belle
$\langle x_p \rangle$	0.5738	0.0061	0.0049	0.0032	0.5824 ± 0.0025
$\langle x_p^2 \rangle$	0.3544	0.0038	0.0030	0.0021	0.3649 ± 0.0034
$\langle x_p^3 \rangle$	0.2305	0.0026	0.0021	0.0015	0.2396 ± 0.0023
$\langle x_p^4 \rangle$	0.1560	0.0020	0.0015	0.0011	0.1630 ± 0.0051
$\langle x_p^5 \rangle$	0.1090	0.0015	0.0012	0.0009	0.1151 ± 0.0020
$\langle x_p^6 \rangle$	0.0783	0.0012	0.0010	0.0008	0.0851 ± 0.0023

TABLE III. Fragmentation models compared with the data. Here $m_\perp^2 = m_H^2 + p_\perp^2$, $p_\perp$ is the component of the hadron momentum transverse to the quark momentum, and the z_i are defined in the text.

Model	$f(z, \beta)$	Ref.
CS	$([1 - z_1]/z_1 + \epsilon[2 - z_1]/[1 - z_1])(1 + z_1^2) \times (1 - 1/z_1 - \epsilon/[1 - z_1])^{-2}$	[5]
BCFY	$z_2(1 - z_2)^2(1 - [1 - d]z_2)^6[3 - 3z_2 \cdot (3 - 4d) + z_2^2 \cdot (12 - 23d + 26d^2) - z_2^3 \cdot (9 - 11d + 12d^2)(1 - d) + 3z_2^4 \cdot (1 - d + d^2)(1 - d)^2]$	[7]
KLP-M	$z_2^\alpha \cdot (1 - z_2)$	[9]
KLP-B	$z_2^\alpha \cdot (1 - z_2)^3$	[13]
Bowler	$z_3^{-(1+bm_\perp^2)}(1 - z_3)^a \exp(-bm_\perp^2/z_3)$	[10]
Peterson	$(1/z_2)(1 - [1/z_2] - \epsilon/[1 - z_2])^{-2}$	[11]
Lund	$(1/z_1)(1 - z_1)^a \exp(-bm_\perp^2/z_1)$	[12]

where n is the number of bins, $P_i^{\rm data}$ ($P_i^{\rm MC}$) is the fraction of the measured (modeled) distribution in bin i, and $\mathbf{V}$ is the full error matrix formed from the errors on the data (Table I) with the statistical errors on the simulation added in quadrature to the diagonal elements. For each function in Table III we minimize this χ^2 with respect to the set of parameters β by scanning over a wide range of possible β values and generating a large sample of $q\bar{q}$ events at each of several points. We then generate additional sets near each minimum. All other model parameters are fixed to their default values.

The functions with one free parameter (CS, BCFY, KLP-M, KLP-B, and Peterson) all show a single, well-behaved minimum. The two parameters in the Bowler and Lund functions are strongly correlated, and the χ^2 shows a single narrow valley. The UCLA model has internal parameters a and b that control production of all particles simultaneously; since it has been suggested that their values should be different for mesons and baryons, we vary them by the same procedure, again finding a strong correlation and a narrow χ^2 valley. HERWIG has no free parameter controlling heavy hadron production, so we consider only the default parameter values.

We compare the fitted distributions with the data in Fig. 8, and list the χ^2, the fitted parameter values and the average x_p of each fitted distribution in Table IV. The parameter values are meaningful only in the context of the JETSET (or UCLA) model. The KLP-B, Lund, and Bowler models give the best descriptions of the data, with respective χ^2 confidence levels of 0.15, 0.11, and 0.06. However their fitted distributions are systematically below the data at the lowest x_p values and above the data just below the peak region. The UCLA distribution is qualitatively similar to these three models but falls more rapidly at low x_p, resulting in poor agreement with the data. The CS, BCFY, and KLP-M models predict distributions that are much too broad, and the Peterson distribution is also too broad. The HERWIG distribution is consistent with the data in the peak region, but cuts off too sharply at high x_p.

The fitted values of the parameter a for the UCLA, JETSET + Lund, and JETSET + Bowler models are larger than those that describe the production of inclusive light hadrons and charmed mesons ($a \approx 1.2$ for UCLA and $0.1 \leq a \leq 0.6$ for the other two models). Differences between baryon and meson distributions have been suggested on the basis of quark counting [13,14]. Crossing of the diagram for leading hadron production in e^+e^- annihilation gives a deep inelastic scattering diagram, calculations for which depend on the number of spectator quarks, N_s; in the limit $z \rightarrow 1$, one expects $f(z) \propto (1 - z)^{2N_s - 1}$ [13,33], and $2N_s - 1 = 3$ for baryons. This is the form of the KLP-B function, which provides a much better description of the data than its counterpart for mesons. The UCLA model and the Lund and Bowler functions also contain $(1 - z)^a$ terms. For UCLA, the fitted value of $a = 2.9$ is close to 3, as anticipated [14].

The models predict $P(x_p)$ for primary leading charmed hadrons, whereas the data also contain secondary charmed hadrons from the splitting of hard gluons, and some of the reconstructed Λ_c^+ are decay products of other charmed baryons. Both of these effects are included in the JETSET, HERWIG, and UCLA models, but it is important to consider the effects of possible mismodelling. The fraction of $q\bar{q}$ events containing a gluon splitting into a $c\bar{c}$ pair has been measured at $\sqrt{s} = 92$ GeV to be about 0.01 [34]. At our lower c.m. energy this rate is expected to be reduced, and the fraction of these that produce charmed baryons is expected to be lower than that for primary c and $\bar{c}$ quarks. The JETSET, UCLA, and HERWIG models predict overall contributions of only $(0.009 \pm 0.004)\%$, $(0.017 \pm 0.005)\%$, and $(0.034 \pm 0.012)\%$, respectively, concentrated at low x_p. The uncertainties in our lowest-x_p bins are large enough to accommodate such a contribution. Adjusting the models to remove or double this contribution does not change the results of the fits significantly.

Currently there are three known Σ_c states (with masses 2455, 2520, and 2880 MeV/c^2) that decay into $\Lambda_c^+\pi$, and four Λ_c states (masses 2593, 2625, 2765, and 2880 MeV/c^2) that decay into $\Lambda_c^+\pi^+\pi^-$. In decays of such baryons into a slightly lighter baryon and one or two pions, the daughter baryon carries most of the momentum, so the effect of any such decay is to soften $P(x_p)$ slightly without distorting it substantially. In the

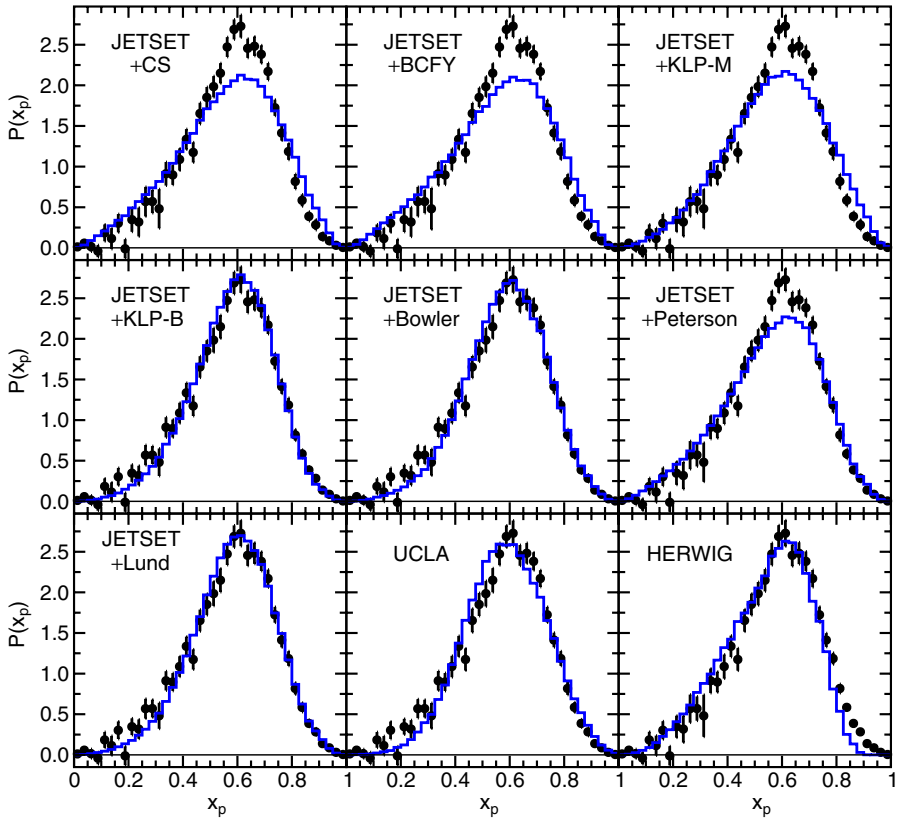

FIG. 8 (color online). The Λ_c^+ x_p distribution (dots) compared with the results of the model tests (histograms) described in the text. The error bars include simulation statistics.

JETSET + Lund, JETSET + Bowler, and UCLA models, this effect is partially compensated by the fact that the heavier baryons are generated with slightly harder distributions. Collectively, the effect is to broaden $P(x_p)$ slightly and shift its average value down. Combining our Λ_c^+ candidates with additional pions in the same event, we see clear signals for all of these states, and can compare the relative contributions to the detected Λ_c^+ with the simulation. The largest contribution of about 7% from $\Sigma_c(2455)$ is well simulated in all models, but the $\Sigma_c(2520)$ rate is too high by a factor of $\sim$3, and the excited Λ_c states are not in any simulation. Removing two-thirds of the $\Sigma_c(2520)$ narrows the simulated distributions slightly, but does not improve any χ^2 value significantly. Similarly, adding excited Λ_c states broadens all distributions slightly, with no change in the conclusions of the model tests. No Ξ_c or Ω_c states are known to decay to Λ_c^+ [4], except two recently reported by Belle [31]. The latter are observed at very low rates, so should have negligible effect on $P(x_p)$.

TABLE IV. Results of the fragmentation model tests. The minimum χ^2 value, number of degrees of freedom, fitted parameter values, and the mean value of the corresponding scaled momentum distribution are listed.

Model	χ^2/dof	Parameters	$\langle x_p \rangle$
JETSET + CS	227/39	$\epsilon = 0.135$	0.563
JETSET + BCFY	234/39	$d = 0.355$	0.560
JETSET + KLP-M	219/39	$\alpha = 3.05$	0.572
JETSET + KLP-B	48/39	$\alpha = 7.62$	0.580
JETSET + Bowler	52/38	$a = 0.93$, $b = 0.88$	0.583
JETSET + Peterson	100/39	$\epsilon = 0.077$	0.559
JETSET + Lund	49/38	$a = 1.20$, $b = 0.71$	0.584
UCLA	107/38	$a = 2.9$, $b = 0.74$	0.584
HERWIG	456/40	-	0.546

VI. RESULTS FOR $\Upsilon(4S)$ DECAYS

A. Charmed baryon production

The differential production rate per $\Upsilon(4S)$ decay is shown in Fig. 9 and listed in Table V. The errors are as for the $q\bar{q}$ results, with an additional 1.5% normalization uncertainty due to the $q\bar{q}$ subtraction procedure. The kinematic limit for $\Upsilon(4S) \to B\bar{B} \to \Lambda_c^+ \bar{p}$ decays is $x_p = 0.47$, and above this value the rate is consistent with zero. This region is omitted from the table and only partly shown in the figure. We calculate the total rate by integrating the differential rate over the kinematically allowed bins. The resulting product of total rate and branching fraction, $N^{\Upsilon}_{\Lambda c} \cdot \mathcal{B}_{pK^-\pi^+} = 4.56 \pm 0.09(\text{stat.}) \pm 0.31(\text{syst.}) \times 10^{-3}$, is consistent with previous measurements [2,24]. It corre-

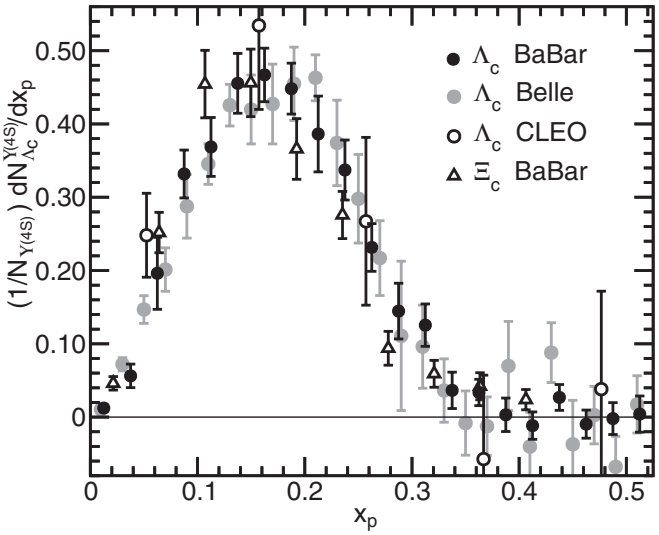

FIG. 9. Differential Λ_c^+ production rate per $\Upsilon(4S)$ decay compared with previous measurements. Normalization errors are not shown, and the Ξ_c^0 rate is normalized to match the peak Λ_c^+ rate.

sponds to $N_{\Lambda c}^{\Upsilon} = 0.091 \pm 0.006$ (exp.) ± 0.024 (BF) Λ_c^+ per $\Upsilon(4S)$ decay, and $4.5 \pm 1.2\%$ of B^0/B^- decays including a Λ_c^+ baryon, assuming the $\Upsilon(4S)$ decays predominantly to $B\bar{B}$.

TABLE V. Λ_c^+ differential production rate per $\Upsilon(4S)$ decay per unit scaled momentum (to $\sqrt{s} = 10.58$ GeV). The last column includes those experimental errors that are correlated between x_p values and affect the shape of the distribution. Normalization uncertainties are given only on the total.

x_p Range	$\frac{1}{N_\Upsilon}\frac{dN_{\Lambda c}^{\Upsilon}}{dx_p}$	Statistical Error	Systematic Independent	Systematic Correlated
0.000–0.025	0.0123	0.0023	0.0040	0.0013
0.025–0.050	0.0563	0.0073	0.0135	0.0046
0.050–0.075	0.1963	0.0110	0.0443	0.0182
0.075–0.100	0.3317	0.0152	0.0194	0.0215
0.100–0.125	0.3686	0.0193	0.0196	0.0294
0.125–0.150	0.4555	0.0208	0.0285	0.0205
0.150–0.175	0.4669	0.0221	0.0238	0.0167
0.175–0.200	0.4482	0.0201	0.0240	0.0151
0.200–0.225	0.3863	0.0211	0.0454	0.0132
0.225–0.250	0.3372	0.0204	0.0339	0.0109
0.250–0.275	0.2315	0.0197	0.0246	0.0084
0.275–0.300	0.1447	0.0183	0.0327	0.0064
0.300–0.325	0.1255	0.0171	0.0227	0.0055
0.325–0.350	0.0365	0.0175	0.0171	0.0041
0.350–0.375	0.0336	0.0160	0.0072	0.0037
0.375–0.400	0.0031	0.0163	0.0155	0.0043
0.400–0.425	−0.0117	0.0163	0.0080	0.0042
0.425–0.450	0.0268	0.0150	0.0081	0.0044
0.450–0.475	−0.0096	0.0158	0.0097	0.0048
Total	0.0910	0.0019	0.0026	0.0049
Norm. error	0.0029			
BF error	0.0237			

Our results on the shape are consistent with, and more precise than, previous results, which are also shown in Fig. 9. The x_p distribution is quite soft. In particular, the data drop rapidly above the peak and are consistent with zero above $x_p \approx 0.35$. This is the range expected for quasi-two-body decays into a Λ_c^+ or Σ_c plus an antibaryon such as a $\bar{p}$, $\bar{n}$, or $\bar{\Delta}$, and includes much of the range expected for decays involving one or two additional pions. The $\bar{B}^0 \to \Lambda_c^+ \bar{p}$ decay has been observed [21] at a very low rate consistent with our inclusive data.

A soft x_p distribution was also seen in our recent study of Ξ_c^0 baryons [3], but the statistics of that study did not allow a meaningful direct subtraction of the contribution from $q\bar{q}$ events. As an exercise, we assume a smooth distribution from $q\bar{q}$ events by choosing an empirical function that describes both the Λ_c^+ data in Sec. V and the high-x_p Ξ_c^0 data [Fig. 7(a)]. We fit this function to the high-x_p Ξ_c^0 data and subtract the result in all x_p bins. The resulting approximate x_p distribution for Ξ_c^0 in $\Upsilon(4S)$ decays is also shown in Fig. 9, normalized to have roughly the same peak height as the Λ_c^+ data. It is also quite soft, similar in shape to the Λ_c^+ but shifted slightly downward in x_p, and consistent with zero above $x_p \approx 0.35$. Because of the $e^+e^- \to c\bar{c}$ subtraction procedure, the error bars cannot be compared with those for the Λ_c^+ data, but the noted features do not depend on the details of the subtraction procedure.

B. Model tests

Existing models of B meson decays into c baryons were developed with little data on the x_p distribution. In Fig. 10(a) we compare $P(x_p)$ (normalized over the range $x_p < 0.475$) with the predictions of the models in the JETSET generator [28] and our internal generator [29]. The former has been tuned to measured multiplicities and momentum distributions of stable B decay products, and predicts a distribution that is much too soft. The latter includes many measured exclusive decays involving D mesons and postulates analogous few-body decays involving charmed baryons. Its predicted x_p distribution is similar in shape to the data, but shifted to higher x_p values. Neither generator produces simple (quasi-)two-body decays such as $B \to \Lambda_c^+ \bar{p}$, $\Lambda_c^+ \bar{n}$, $\Lambda_c^+ \bar{\Delta}$, or $\Sigma_c \bar{p}$.

In Fig. 10(b) we compare the same data with simulated events of the type $B \to \Lambda_c^+ \bar{p}(m\pi)$ for selected values of m, the number of pions in the decay in addition to the Λ_c^+ and antiproton. The distributions are insensitive to the charges of the pions or B meson, or to replacing the antiproton with an antineutron. Decays via a $\bar{\Delta}$ or strange antibaryon are not included; they give Λ_c^+ distributions only slightly different from those shown with $m - 1$ pions. For $m = 1$, 2, 4, and 6, the distributions shown are from the JETSET

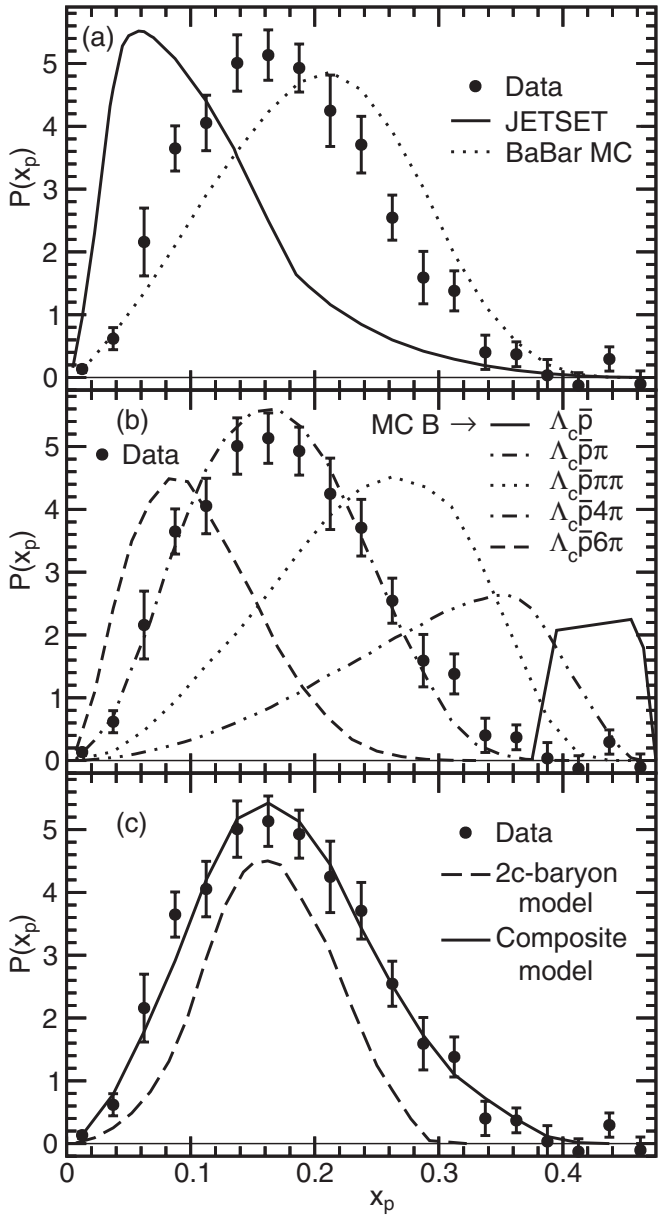

FIG. 10. $P(x_p)$ for Λ_c^+ from $\Upsilon(4S)$ decays (dots) compared with the simulations (lines) described in the text. The data are normalized to unit area, as are the *BABAR* simulation in (a), the $B \to \Lambda_c^+ \bar{p} 4\pi$ simulation in (b), and the composite simulation in (c); all other simulations are normalized arbitrarily.

simulation; phase space decays give similar distributions. The spread in the distribution for $m = 0$ is due to the finite momentum of the B meson in the e^+e^- c.m. frame. The measured $P(x_p)$ is described adequately by the simulation with $m = 4$. Adding contributions from $m = 3$ and $m = 5$ improves the χ^2 of a comparison with the data, but no further contributions are helpful. That m is restricted to such a narrow range suggests that different types of decay modes are needed.

An intriguing possibility is that there is a large contribution from decays involving both a c baryon and an anti-c baryon. The decays $\bar{B}^0 \to \Xi_c^+ \bar{\Lambda}_c^-$ [22] and $B^- \to \Lambda_c^+ \bar{\Lambda}_c^- K^-$ [23] have recently been observed, and we have previously measured an unexpectedly high rate of inclusive $\bar{\Lambda}_c^-$ in B^- decays [20]. As an exercise, we model two-body two-c-baryon decays based on the simplest internal W diagrams, i.e. those of the forms $B^- \to \Xi_c^+(\Lambda_c^+)\bar{\Sigma}_c^{--}$, $B^- \to \Xi_c^0(\Sigma_c^0)\bar{\Lambda}_c^-$, $\bar{B}^0 \to \Xi_c^+(\Lambda_c^+)\bar{\Lambda}_c^-$, and $\bar{B}^0 \to \Xi_c^0(\Sigma_c^0)\bar{\Sigma}_c^0$, where the parentheses indicate Cabibbo-suppressed modes. Here, Ξ_c represents any of the states $\Xi_c(2470)$, $\Xi_c'(2570)$, or $\Xi_c(2645)$, Σ_c represents $\Sigma_c(2455)$ or $\Sigma_c(2520)$, Λ_c represents $\Lambda_c(2285)$, $\Lambda_c(2593)$, or $\Lambda_c(2625)$, and we consider all kinematically allowed combinations at relative rates determined by phase space. We decay all Σ_c baryons into $\Lambda_c^+\pi$ and all excited Λ_c baryons into $\Lambda_c^+\pi\pi$, with 73% of the $\Lambda_c^+(2593)$ baryons decaying through a $\Sigma_c\pi$ intermediate state and all others via phase space.

The x_p distribution of the Λ_c^+ from this simulation is compared with the data in Fig. 10(c). Although it is too narrow to describe the data completely, it appears that such processes could contribute substantially to the overall rate. Combining this simulation with those for the $B \to \Lambda_c^+ \bar{p}(m\pi)$ modes and assuming a smooth, broad distribution of m, we can describe the data with as much as a 50% contribution from these two-c-baryon decays. For example, the "composite model" in Fig. 10(c) comprises 35% two-c-baryon decays and (12, 25, 12, 9, 7)% of $m =$ (2, 3, 4, 5, 6), and provides an excellent description of the data. Decays with two charmed baryons and additional pions or kaons could also contribute at low x_p, shifting the m distribution downward. Measurements of many exclusive baryonic B decays, including both one- and two-c-baryon modes, are needed to understand the dynamics in detail.

VII. SUMMARY AND CONCLUSIONS

We use the excellent tracking and particle identification capabilities of the *BABAR* detector to reconstruct large, clean samples of Λ_c^+ baryons over the full kinematic range. We measure their total production rates and inclusive scaled momentum distributions in both $e^+e^- \to$ hadrons events at $\sqrt{s} = 10.54$ GeV and $\Upsilon(4S)$ decays. Our results are consistent with those published previously and more precise.

In $e^+e^- \to q\bar{q}$ events we measure a total rate per event times branching fraction into the $pK^-\pi^+$ mode of

$$N_{\Lambda c}^{q\bar{q}} \cdot \mathcal{B}_{pK^-\pi^+} = 2.84 \pm 0.04(\text{stat.}) \pm 0.09(\text{syst.}) \times 10^{-3},$$

where the first error is statistical and the second systematic. The uncertainty on the total rate per $q\bar{q}$ event, $N_{\Lambda c}^{q\bar{q}} = 0.057 \pm 0.002(\text{exp.}) \pm 0.015$ (BF), is dominated by the uncertainty on $\mathcal{B}_{pK^-\pi^+}$. The corresponding value of $N_{\Lambda c}^{c} = 0.071 \pm 0.003(\text{exp.}) \pm 0.018$ (BF) Λ_c^+ per c-quark jet is

consistent with the hypothesis that roughly 10% of c jets produce a c baryon and a large fraction of these decay via a Λ_c^+.

The scaled momentum distribution peaks at $x_p \approx 0.6$. It is similar in shape to those measured previously for D and D^* mesons, but peaks more sharply and drops toward zero more rapidly as $x_p \to 1$. We measure an average value for Λ_c^+ of

$$\langle x_p \rangle = 0.574 \pm 0.006(\text{stat.}) \pm 0.006(\text{syst.}),$$

which is consistent with values measured for ground state D mesons, but about 5% lower than those for D^* mesons. We use this distribution to test several models of heavy-quark fragmentation, none of which provides a complete description of the data. The baryon-specific model of Kartvelishvili *et al.* and the models of Lund and Bowler have acceptable χ^2 values, but all show a steeper slope on the low side of the peak than the data. The UCLA model shows similar qualitative features, but worse agreement with the data. The HERWIG model is far too narrow, and all others are too broad. In previous model tests using specific c mesons [2] and inclusive b hadrons [16] (a mix of roughly 90% mesons and 10% baryons), the Lund, Bowler, and Kartvelishvili models generally gave the best description of the data, and UCLA described the b-hadron data, whereas the other models showed discrepancies similar in form to those reported here. The Kartvelishvili and UCLA models postulate different spectra for mesons and baryons. Their strong preference for their respective baryonic forms, combined with the observed differences in shape between our Λ_c^+ spectrum and previously measured D meson spectra, indicate a difference in the underlying dynamics.

In $\Upsilon(4S)$ decays, we measure a total rate per event times branching fraction of

$$N_{\Lambda c}^{\Upsilon} \cdot \mathcal{B}_{pK^-\pi^+} = 4.56 \pm 0.09(\text{stat.}) \pm 0.31(\text{syst.}) \times 10^{-3},$$

corresponding to $N_{\Lambda c}^{B} = 0.045 \pm 0.003$ (exp.) ± 0.012 (BF) per $\bar{B}^0/B^-$ decay. The spectrum is softer than predicted by our B decay model, and much harder than that predicted by JETSET. It can be described by models of $B \to \Lambda_c^+ \bar{p}(m\pi)$ decays only if the $m = 3$–5 contributions dominate. Alternatively, a model including a large contribution from decays involving both a charmed and an anti-charmed baryon can describe the data in conjunction with a broad distribution of m. Additional studies of exclusive modes are needed to understand the details of B-meson decays into baryons.

ACKNOWLEDGMENTS

We are grateful for the extraordinary contributions of our PEP-II colleagues in achieving the excellent luminosity and machine conditions that have made this work possible. The success of this project also relies critically on the expertise and dedication of the computing organizations that support *BABAR*. The collaborating institutions wish to thank SLAC for its support and the kind hospitality extended to them. This work is supported by the U.S. Department of Energy and National Science Foundation, the Natural Sciences and Engineering Research Council (Canada), Institute of High Energy Physics (China), the Commissariat à l'Energie Atomique and Institut National de Physique Nucléaire et de Physique des Particules (France), the Bundesministerium für Bildung und Forschung and Deutsche Forschungsgemeinschaft (Germany), the Istituto Nazionale di Fisica Nucleare (Italy), the Foundation for Fundamental Research on Matter (The Netherlands), the Research Council of Norway, the Ministry of Science and Technology of the Russian Federation, Ministerio de Educación y Ciencia (Spain), and the Particle Physics and Astronomy Research Council (United Kingdom). Individuals have received support from the Marie-Curie IEF program (European Union) and the A. P. Sloan Foundation.

[1] M. Artuso *et al.* (CLEO Collaboration), Phys. Rev. D **70**, 112001 (2004).
[2] R. Seuster *et al.* (Belle Collaboration), Phys. Rev. D **73**, 032002 (2006).
[3] B. Aubert *et al.* (*BABAR* Collaboration), Phys. Rev. Lett. **95**, 142003 (2005).
[4] W. M. Yao *et al.* (Particle Data Group), J. Phys. G **33**, 1 (2006).
[5] P. D. B. Collins and T. P. Spiller, J. Phys. G **11**, 1289 (1985).
[6] B. Mele and P. Nason, Phys. Lett. B **245**, 635 (1990); Nucl. Phys. **B361**, 626 (1991); G. Colangelo and P. Nason, Phys. Lett. B **285**, 167 (1992).
[7] E. Braaten, K. Cheung, and T. C. Yuan, Phys. Rev. D **48**, R5049 (1993); E. Braaten, K. Cheung, S. Fleming, and T. C. Yuan, Phys. Rev. D **51**, 4819 (1995).
[8] Yu. L. Dokshitzer, V. A. Khoze, and S. I. Troyan, Phys. Rev. D **53**, 89 (1996).
[9] V. G. Kartvelishvili, A. K. Likhoded, and V. A. Petrov, Phys. Lett. B **78**, 615 (1978).
[10] M. G. Bowler, Z. Phys. C **11**, 169 (1981).
[11] C. Peterson, D. Schlatter, I. Schmitt, and P. M. Zerwas, Phys. Rev. D **27**, 105 (1983).
[12] B. Andersson, G. Gustafson, G. Ingelman, and T. Sjöstrand, Phys. Rep. **97**, 31 (1983).
[13] V. G. Kartvelishvili and A. K. Likhoded, Sov. J. Nucl.

Phys. **29**, 390 (1979).
[14] S. Chun and C. Buchanan, Phys. Rep. **292**, 239 (1998).
[15] R. L. Jaffe and L. Randall, Nucl. Phys. **B412**, 79 (1994); L. Randall and N. Rius, Nucl. Phys. **B441**, 167 (1995).
[16] G. Abbiendi *et al.* (OPAL Collaboration), Eur. Phys. J. C **29**, 463 (2003); K. Abe *et al.* (SLD Collaboration), Phys. Rev. D **65**, 092006 (2002); A. Heister *et al.* (ALEPH Collaboration), Phys. Lett. B **512**, 30 (2001).
[17] M. Acciari *et al.* (L3 Collaboration), Phys. Lett. B **465**, 323 (1999); K. Ackerstaff *et al.* (OPAL Collaboration), Z. Phys. C **74**, 413 (1997); D. Buskulic *et al.* (ALEPH Collaboration), Z. Phys. C **69**, 393 (1996); P. Abreu *et al.* (DELPHI Collaboration), Phys. Lett. B **345**, 598 (1995).
[18] G. Alexander *et al.* (OPAL Collaboration), Z. Phys. C **72**, 1 (1996); D. Buskulic *et al.* (ALEPH Collaboration), Z. Phys. C **62**, 1 (1994); P. Abreu *et al.* (DELPHI Collaboration), Z. Phys. C **59**, 533 (1993).
[19] P. Avery *et al.* (CLEO Collaboration), Phys. Rev. D **43**, 3599 (1991).
[20] B. Aubert *et al.* (*BABAR* Collaboration), Phys. Rev. D **70**, 091106 (2004); hep-ex/0606026.
[21] N. Gabyshev *et al.* (Belle Collaboration), Phys. Rev. Lett. **90**, 121802 (2003).
[22] R. Chistov *et al.* (Belle Collaboration), hep-ex/0510074.
[23] N. Gabyshev *et al.* (Belle Collaboration), hep-ex/0508015.
[24] G. D. Crawford *et al.* (CLEO Collaboration), Phys. Rev. D **45**, 752 (1992).
[25] B. Aubert *et al.* (*BABAR* Collaboration), Nucl. Instrum. Methods Phys. Res., Sect. A **479**, 1 (2002).
[26] B. L. Hartfiel, Ph.D. thesis, University of California-Los Angeles, 2005; SLAC-R-823.
[27] S. Agostinelli *et al.* (GEANT4 Collaboration), Nucl. Instrum. Methods Phys. Res., Sect. A **506**, 250 (2003).
[28] T. Sjöstrand, Comput. Phys. Commun. **135**, 238 (2001).
[29] D. J. Lange, Nucl. Instrum. Methods Phys. Res., Sect. A **462**, 152 (2001).
[30] B. Aubert *et al.* (*BABAR* Collaboration), Phys. Rev. D **72**, 052006 (2005).
[31] R. Chistov *et al.* (Belle Collaboration), Phys. Rev. Lett. **97**, 162001 (2006).
[32] G. Marchesini *et al.*, Comput. Phys. Commun. **67**, 465 (1992).
[33] R. Gatto, P. Menotti, and I. Vendramin, Phys. Rev. D **7**, 2524 (1973).
[34] A. Heister *et al.* (ALEPH Collaboration), Phys. Lett. B **561**, 213 (2003); M. Acciari *et al.* (L3 Collaboration), Phys. Lett. B **476**, 243 (2000); G. Abbiendi *et al.* (OPAL Collaboration), Eur. Phys. J. C **13**, 1 (2000).